

## Electrical and Magnetic Properties of La(Ba)MnO<sub>3</sub> Thin Films

Tamio Endo<sup>1,2)</sup>, Shin-ichi Iwasaki<sup>1)</sup>, Kouji Yoshii<sup>1)</sup>, Takahisa Sakurada<sup>1)</sup>, Michi Ogata<sup>1)</sup>,  
Ajay K. Sarkar<sup>1)</sup>, Josep Nogues<sup>3)</sup>, Juan S. Munoz<sup>3)</sup>, Jose Colino<sup>4)</sup>

- 1) Faculty of Engineering, Mie University, Tsu, Mie 514-8507, Japan  
T. Endo: endo@elec.mie-u.ac.jp
- 2) National Institute of Advanced Industrial Science and Technology (AIST), Tsukuba, Ibaraki 305-8568, Japan
- 3) ICREA and Dept. de Fisica, Universitat Autònoma de Barcelona, 08193 Bellaterra, Spain
- 4) Departamento de Fisica Aplicada, Universidad de Castilla-La Mancha, Campus Universitario, 13071 Ciudad Real, Spain

A device concept of tunable microwave filter consisting of a double layer of high temperature superconducting and ferromagnetic layers, is described. La(Ba)MnO<sub>3</sub> thin films are fabricated. The film has a metal-insulator transition temperature of 82.2 K, and a Curie temperature of 140 K. Then the film is insulating and ferromagnetic in 82.2-140 K. Origins are discussed in terms of phase separation.

Key words: Manganite LBMO Thin Films, Ion Beam Sputtering, SQUID Magnetization, Magnetoresistance, Phase Separation,

### 1. Introduction

High temperature superconducting (HTS) microwave filters are most expected since these devices may be used at base stations of mobile communication system. Currently dielectric resonators are used as the microwave filters at most of the base stations. Such filters, however, have large insertion losses then high power amplification of signals is required after the filtering. Furthermore, a skirt performance of the filters is not so good. Though, the numbers of mobile phones must be increased a lot, in addition, higher grade of functions are expected much in the near future. To realize these, such problems must be solved. A downsizing of the device is also an important factor, because there is no space for the large base stations in big cities. If the insertion loss is reduced, it can contribute to the energy saving owing to the lower power amplification.

### 2. HTS Tunable Microwave Filter

The HTS microwave filters can solve these problems [1-3]. Basically the HTS thin film is fabricated into a strip line, then a resonating microwave with a wavelength equal to the strip line length can be transmitted. In this filter, the microwave propagates on the superconducting thin film which has very low surface resistance. Therefore, the HTS filters have extremely low insertion loss and fine skirt performance. The total size can be reduced using excellent cryo-coolers, leading to the solution of crowded base stations. A part of base stations are already employing the HTS filters in USA.

We have a demand to obtain tunable filters which are widely applicable for various mobile phone systems.

This leads to high efficiency of the production and energy conservation. Now we have two ideas for the tunable filters. One is a stacking of HTS film layer on ferroelectric layer [4]. The other is a stacking of HTS film layer on ferromagnetic layer as shown in Fig.1 [5]. When magnetic field is applied, a permeability ( $\mu$ ) of the ferromagnetic layer is modified then the microwave propagation mode (velocity) on the HTS layer is modified accordingly. It results in the shift of center frequency ( $f_0$ ) as

$$f_0 = n \frac{c}{2L\sqrt{\epsilon\mu}}, \quad (1)$$

where  $n$  is order of resonant wavelength,  $c$  light velocity,  $L$  strip line length, and  $\epsilon$  dielectric constant of medium.

### 3. Key Factors for Tunable Filter

The HTS layer must satisfy several demands. A superconducting critical temperature  $T_{cr}$  must be higher. Because we can set a device temperature  $T_d$  higher ( $T_d < T_{cr}$ ). This is an important factor in terms of the cryo-cooler power consumption. Further, if  $T_{cr}$  is higher, the surface resistance of HTS layer is lower at  $T_d$ . Therefore, the microwave surface resistance should be absolutely low [2,6]. If it is high, the microwave is absorbed in the HTS layer, leading to the larger insertion loss. Surface roughness of the HTS layer is also very important factor because it causes microwave scattering. The resonant standing wave is affected by the surface roughness then characteristics of narrow band-width and sharp skirt-cut are degraded. Therefore it is strictly important to obtain the smooth double layer. The factors which affect the surface resistance of HTS

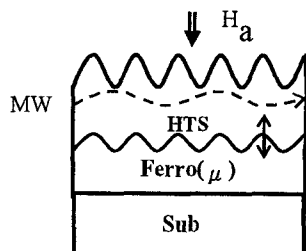


**Fig.1** Schematic diagram of HTS/Ferro double layer. A straight arrow indicates the interdiffusion. A dashed wave indicates the microwave propagation. Sub: substrate.

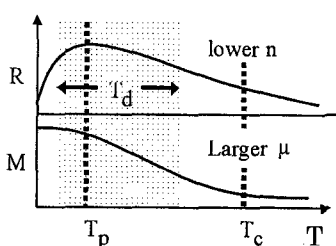


**Fig.2** Schematic diagram of resistance (R) and magnetization (M) vs temperature (T) for the ferromagnetic layer.  $n$ : carrier density. See text for other symbols.

(YBa<sub>2</sub>Cu<sub>3</sub>O<sub>x</sub>) layer are crystal defects such as a-c phase boundaries, twin boundaries, grain boundaries and any other point defects [7-10]. In this paper, we do not mention on these subjects of YBa<sub>2</sub>Cu<sub>3</sub>O<sub>x</sub> layer any more. The details are referred in ref.8.

We mention here on important factors of the ferromagnetic layer (Ferro) and the double layer of HTS/Ferro. First, interdiffusions of both elements as shown in Fig.1 are always fundamental problem in the stacking deposition. One of basic solutions is a low temperature deposition. The second, the surface roughness must be especially reduced in the deposition procedure of Ferro → HTS. Because, if the surface roughness of underlying Ferro layer is large, it must be enhanced in the process of the overlying HTS layer. In this case, the low temperature process is also desirable since it can bring the smooth surface. However, we have to keep the good crystallinity of both layers even by the low temperature depositions. Then, it is quite necessary to make use of other energies than thermal energy during the depositions.

Let us think of the important properties which Ferro layer should furnish. The permeability must be large because we can induce its large modification by applying small magnetic field. The most difficult

demand is that Ferro layer must be insulating though it is ferromagnetic as illustrated in Fig.2. Because, if it is metallic, the microwave is absorbed due to high density carriers. If perovskite manganites are used for Ferro layer, it is very difficult to satisfy these two properties simultaneously. Usually when the phase of manganite colossal magnetoresistance materials is changed from paramagnetic to ferromagnetic with decreasing temperature (T), it is changed from insulating to metallic due to the "double exchange coupling" (DEC). This is surely very difficult in bulk crystals. However, in case of thin films, there is some possibility that the metal-insulator transition temperature ( $T_p$ ) and the ferromagnetic-paramagnetic transition temperature (Curie temperature  $T_c$ ) are slightly separated. If it is realized, we can obtain the Ferro layer with insulating property at  $T_d$ . Then the condition required to the characteristic temperatures for the double layer is shown as  $T_p < T_d < T_c$  ( $T_{cr}$ ), (see Fig.2).

#### 4. Experimental

We selected La<sub>0.7</sub>Ba<sub>0.3</sub>MnO<sub>3</sub> as the manganite ferromagnetic layer because its intrinsic  $T_c$  is very high. LBMO (La-Ba-Mn-O) thin films were deposited on MgO (100) and LaAlO<sub>3</sub> (LAO) (100) substrates by ion beam sputtering [11]. A target was sputtered by Ar<sup>+</sup> ion beam. The substrates were heated and substrate temperature ( $T_s$ ) was monitored. Oxygen plasma (PL) was supplied, and the oxygen partial pressure ( $P_o$ ) was adjusted.

Crystallinity of LBMO thin films was estimated by X-ray diffraction (XRD). Electrical resistance (R) was measured on the films at various T by four-probe method, and magnetoresistance (MR) was measured under magnetic field ( $H_a$ ) for  $H_a \perp$  plane. Magnetization (M) was measured using SQUID magnetometer for  $H_a \perp$  plane. A part of the samples were annealed at 900°C for 5 h in 1 atom oxygen atmosphere.

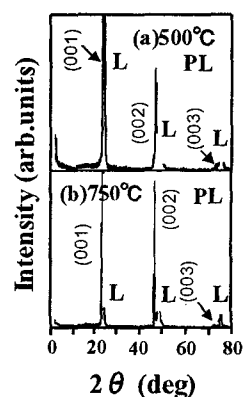


**Fig.3** Typical XRD patterns of LBMO thin films deposited on LAO at (a)  $T_s=500^\circ\text{C}$ ,  $P_o=1\text{mTorr}$  (S-1) and (b)  $T_s=750^\circ\text{C}$ ,  $P_o=0.5\text{mTorr}$  (S-2). L: LAO peak.

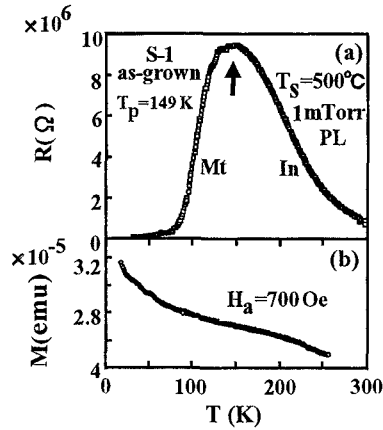


Fig.4 (a) R-T and (b) M-T curves for S-1 (500°C). The film is paramagnetic or weak ferromagnetic.

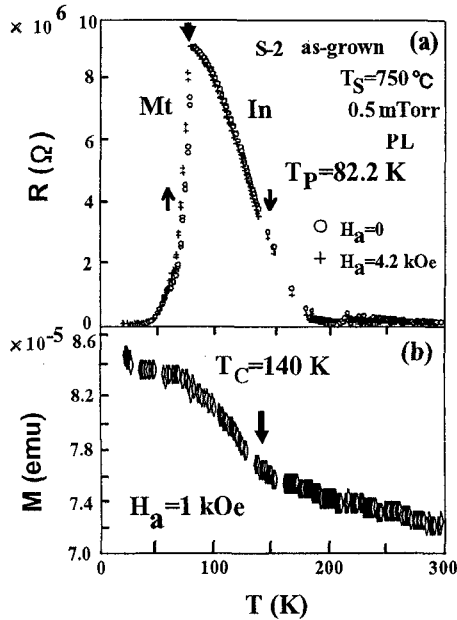


Fig.5 (a) R-T and (b) M-T curves for S-2 (750°C). The values of  $R$  are plotted under  $H_a = 0$  and 4.2 kOe.

5. Results

Excellent crystalline LBMO thin films could be grown at various  $T_S$  from 750°C down to 650°C on MgO while down to 480°C on LAO at various  $P_O$ . This difference is caused by lattice mismatching for MgO and lattice matching for LAO [12-14]. Typical XRD patterns are shown in Fig.3 (a) for  $T_S = 500^\circ\text{C}$  and (b) for  $T_S = 750^\circ\text{C}$ . Single phases of cubic perovskite crystalline films are grown.

We show the results of R-T and M-T in Fig.4 (a) and (b) for the film (S-1) deposited at 500°C. With decreasing  $T$ , the R-T shows insulator to metal (In→Mt)

transition at  $T_P = 149$  K. There is, however, no paramagnetic to ferromagnetic (PM→FM) transition in the M-T in the measured  $T$  range. Usually the In→Mt transition is explained by the DEC theory for the manganites but it must be accompanied by the PM→FM transition [15-17]. Then this In→Mt transition cannot be explained merely by the DEC model.

Next, we show the R-T and M-T in Fig.5 (a) and (b) for the film (S-2) deposited at 750°C. With decreasing  $T$ , the R-T shows the In→Mt transition again at  $T_P = 82.2$  K. This film shows the PM→FM transition at a Curie temperature  $T_C = 140$  K. However,  $T_C$  does not correspond to  $T_P$ , then these two transitions cannot be explained merely by the DEC again. But anyway, we could obtain the film which has the characteristic

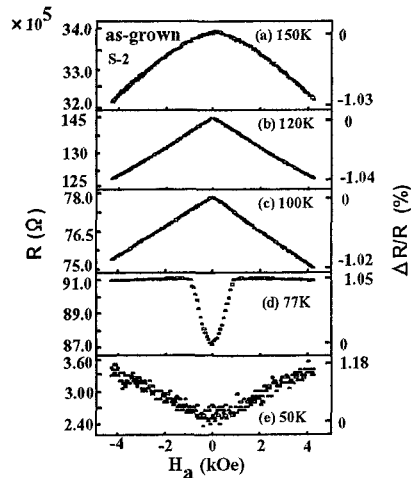


Fig.6 MR vs  $H_a$  at various  $T$  for S-2.

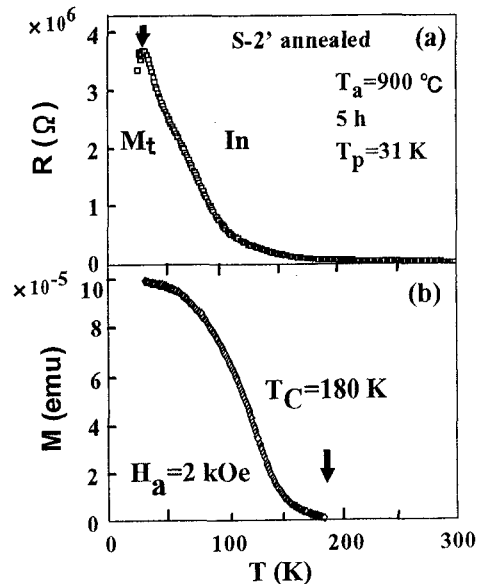


Fig.7 (a) R-T and (b) M-T curves for the annealed sample S-2'.

temperatures of  $T_P < T_C$ , that is, the film is insulating and ferromagnetic in 82.2-140 K.

Carefully watching the R-T curves, they show negative MR effect in the In-regime while positive MR effect in the Mt-regime. Then we measured MR in more detail, the results are shown in Fig.6. In higher temperature regions of the In-regime, it clearly shows the negative MR which is explained by the DEC. Whereas in lower temperature regions of the Mt-regime, it clearly shows the positive MR which cannot be explained by the DEC.

The value of  $T_P=82.2$  K is not sufficiently low for the double layer of HTS/Ferro tunable filter because the HTS layer should have  $T_C$  higher than 82.2 K. This is not easily achieved. Then we tried to anneal this film at 900°C. The results of R-T and M-T after the annealing (S-2') are shown in Fig.7 (a) and (b). The  $T_P$  is shifted to lower T of 31 K, while  $T_C$  is shifted to 180 K in the opposite direction. Then the film is insulating and ferromagnetic in 31-180 K. The  $T_P=31$  K is sufficiently low and  $T_C=180$  K is sufficiently high for the HTS layer, then this ferromagnetic layer can basically be used for the HTS/Ferro tunable filter at the device temperature  $T_d$  between 31 and 180 K.

The as-grown S-2 sample showed the curious MR effect as shown in Fig.6. Therefore we examined MR ratio ( $\Delta R/R$ ) also on this annealed sample S-2', the results are shown in Fig.8 (a). The amount of  $\Delta R/R$  is plotted in Fig.8 (b) as a function of T at a fixed  $H_a=4$  kOe. At the all T, it shows only the negative MR down to 50 K, though the S-2 sample shows the positive MR at the same T. That is, the positive MR disappeared by the annealing. The MR ratios are small at lower T, increase and decrease with increasing T, showing the maximum at  $T=125$  K. The maximum ratio is 17% for  $H_a=4$  kOe. It should be noted that even the sample shows only the negative MR in the measured T region, it is insulating, not metallic. Thus it still violates from the DEC model.

## 6. Discussion

Generally the negative MR in the manganites is interpreted by the DEC model as schematically shown in Fig.9 (a). At high temperatures, localized spins ( $t_{2g}$ ) are fluctuated, then a traveling electron spin ( $e_g$ ) is scattered by these random spins, leading to high resistive insulating (In) nature. Whereas, at low temperatures, the localized spins are aligned, then the traveling electron spin is not scattered by these aligned spins, leading to high conductive metallic (Mt) nature. This is the mechanism why the In $\rightarrow$ Mt and PM $\rightarrow$ FM transitions occur simultaneously with decreasing T.

Our results (Figs.4, 5 and 7) do not obey this rule, then we have two possibilities. The first is that the grown films have different nature from the ordinary manganite nature. Sometimes the positive MR is found

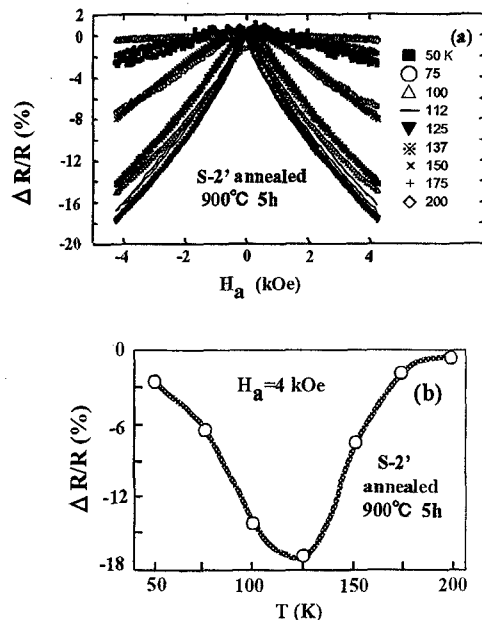


Fig.8 (a) MR vs  $H_a$  and (b)  $\Delta R/R$  vs T at  $H_a=4$  kOe for S-2'.

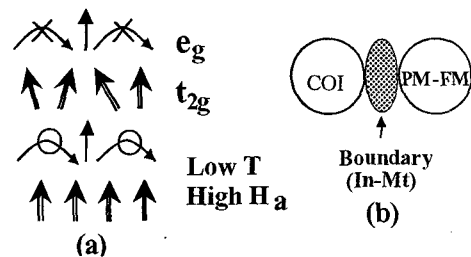


Fig.9 (a) Double exchange coupling model. (b) Phase separation model. PM: paramagnetic, FM: ferromagnetic, COI: charge ordered insulating. The boundary changes between insulating (In) and metallic (Mt) phases following temperature and magnetic field.

on the manganites, and it is explained in terms of "superexchange interaction" [18], "domain structures" [19] and other models [20]. But it is very difficult to interpret all the results by a particular nature at present. Then we try to interpret the results by the second possibility in a framework of the DEC, and employing phase separation.

Let us consider the results on the S-2 sample shown in Fig.5 using the "phase separation model" [21] as shown schematically in Fig.9 (b). With decreasing T, the PM $\rightarrow$ FM transition takes place following the DEC inside "PM-FM phase" grains, then the film shows a kink in the M-T curve at  $T_C=140$  K. At the same time, the In $\rightarrow$ Mt transition should take place. But the PM-FM

grains are surrounded by “charge ordered insulating (COI) phase” grains and grainboundaries. Therefore the high conductive pass is not connected at  $T_C$ . Thus the film is still insulating. The resistance increase is dominated by these insulating regions. With further decreasing  $T$ , the PM-FM grains are extended or the COI grains shrink due to phase change from insulating to metallic nature of the grainboundary. This results in the connection of metallic PM-FM grains then the In  $\rightarrow$  Mt transition of the film takes place at the lower temperature of  $T_P=82.2$  K.

The negative MR (Fig.6) in the In-regime is caused by the ordinary DEC inside the metallic phase of PM-FM grains. Whereas in the In  $\rightarrow$  Mt transition temperature region below  $T_P=82.2$  K, the magnetic field-induced DEC becomes less effective due to well aligned spins while the In  $\rightarrow$  Mt change of the grainboundary is suppressed by the magnetic field application (hypothesis). This results in the positive MR in the Mt-regime (exactly speaking, in the In  $\rightarrow$  Mt transition regime) as shown in Fig.6 (d) and (e). Thus at the boundary temperature between the negative and positive MR regimes, the MR ratio is very small as shown in Fig.6 (c) for  $T=100$  K due to the cancellation. A saturated behavior at 77 K indicates that small amount of metallic elements are exhausted for the Mt  $\rightarrow$  In change by the magnetic field at  $H_a=1$  kOe. Whereas at 50 K, there is no saturation by the field, indicating that there are sufficient amount of metallic elements due to the strong In  $\rightarrow$  Mt change at the well low  $T$ .

As shown in Fig.4, the sample S-1 does not show the conspicuous ferromagnetic nature even though the In  $\rightarrow$  Mt transition takes place at  $T_P=149$  K, because the PM  $\rightarrow$  FM transition in the PM-FM grains may take place at much lower  $T$ . In this case, the PM-FM grains should be “weak metallic” paramagnetic. Then the In  $\rightarrow$  Mt transition of the film is caused by the grainboundary phase change in this sample as well. Alternative explanation is possible. The PM-FM grains may be “weak ferromagnetic” metal in this temperature range. The PM  $\rightarrow$  FM transition takes place at higher temperature around 250 K or more. This can be confirmed if the MR in this temperature range shows negative, but unfortunately we have not measured yet.

The annealed sample S-2' shows the similar behaviors of R-T and M-T (Fig.7) to the sample S-2. Then basically the same interpretation can be applicable. Differences are that the PM  $\rightarrow$  FM transition takes place at the higher  $T_C=180$  K due to enhanced ferromagnetic nature of the PM-FM grains, and that the In  $\rightarrow$  Mt change of the grainboundary takes place at much lower  $T_P=31$  K by the annealing. The negative MR (Fig.8) is caused by the DEC inside the PM-FM grains in the FM temperature range of  $T<180$  K (Fig.7 (b)). Thus the MR effect is absent for  $T=200$  K and negligible for  $T=175$  K

as observed in Fig.8 (b). At  $T=50$  K, the MR effect is small again. This is explained by the two mechanisms as mentioned above already. The positive MR might take place when  $T$  is decreased below  $T_P=31$  K. The 50 K is near the cross over temperature between the negative and positive MR regimes. The other origin is that the localized spins are already well aligned at well low  $T$  of 50 K, therefore the magnetic field has less effect on the further spin alignment.

## 7. Summary

It is described on the HTS microwave filter and HTS/Ferro tunable filter. The LBMO film deposited at 500°C shows very high  $T_P$  (149 K) and very weak ferromagnetic nature. The film deposited at 750°C shows rather low  $T_P$  of 82.2 K and stronger ferromagnetic nature with rather high  $T_C$  of 140 K. This film is hopeful for the Ferro layer, because it is insulating and ferromagnetic. These characteristic temperatures can be improved by the annealing, resulting in  $T_P=31$  K and  $T_C=180$  K. Therefore it can be used as the Ferro layer combined with the HTS layer because  $T_P$  is well below  $T_C$  of HTS.

The origins are discussed for the separated  $T_P$  and  $T_C$ , and for the negative and positive MR. It can be interpreted by one of the hypotheses, phase separation, employing the ordinary DEC model.

## References

- [1] A. T. Findikoglu, Q. X. Jia, X. D. Wu, G. J. Chen, T. Venkatesan, D. W. Reagor, *Appl. Phys. Lett.* 68-12 (1996) 1651.
- [2] A. Lauder, K. E. Myers, D. W. Face, *Adv. Mater.* 10-15 (1998) 1249.
- [3] Z-Y. Shen, C. Wilker, P. Pang, D. W. Face, C. F. Carter III, C. M. Harrington; *IEEE Trans. Appl. Supercond.* 7-2 (1997) 2446.
- [4] S. Hontsu, H. Nishikawa, H. Nakai, J. Ishii, M. Nakamori, A. Fujimaki, Y. Noguchi, H. Tabata, T. Kawai; *Supercond. Sci. Technol.* 12 (1999) 836.
- [5] J. Wosik, L. -M. Xie, M. Strikovski, J. H. Miller Jr., P. Przyslupski; *Appl. Phys. Lett.* 74-5 (1999) 750.
- [6] Z-Y. Shen, F. M. Pellicone, R. J. Small, S. P. McKenna, S. Sun, P. J. Martin; *IEEE Trans. Appl. Supercond.* 7-2 (1997) 1283.
- [7] T. Endo, K. Yoshii, S. Iwasaki, H. Kohmoto, H. Saratani, S. Shiomi, M. Matsui, Y. Kurosaki; *Supercond. Sci. Technol.* 16 (2003) 110.
- [8] T. Endo, H. Kohmoto, S. Iwasaki, M. Matsuo, M. Matsui, Y. Kurosaki, H. Nakanishi, K. Niwano; *New Materials*, eds. P. Rama Rao, M. Doyama etc. (ARCI and JSPS, 2003) pp. 205-223, (*Proc. Asia Academic Seminar on New Materials*, Hyderabad, 2001).

- [9] T. Endo, KI. Itoh, A. Hashizume, H. Kohmoto, E. Takahashi, D. Morimoto, V. V. Srinivasu, T. Masui, K. Niwano, H. Nakanishi; *J. Crystal Growth* 229 (2001) 321.
- [10] T. Endo, KI. Itoh, M. Horie, KT. Itoh, N. Hirate, S. Yamada, M. Tada, S. Sano; *Physica C* 333 (2000) 181.
- [11] T. Endo, H. Yan, M. Wakuta, H. Nishiku, M. Goto; *Jpn. J. Appl. Phys.* 35-10 (1996) L1260.
- [12] M. Tada, J. Yamada, V. V. Srinivasu, V. Sreedevi, H. Kohmoto, A. Hashizume, Y. Inamori, T. Tanaka, A. Harrou, J. Nogues, J. S. Munoz, J. M. Colino, T. Endo; *J. Crystal Growth* 229 (2001) 415.
- [13] J. Yamada, M. Tada, H. Kohmoto, A. Hashizume, Y. Inamori, D. Morimoto, T. Endo, J. M. Colino, J. Santamaria; *Trans. Mat. Res. Soc. Jpn.* 26-3 (2001) 1053.
- [14] J. Yamada, M. Tada, A. Hashizume, H. Kohmoto, E. Takahashi, S. Shiomi, T. Endo, J. Nogues, J. S. Munoz, T. Masui; *Trans. Mat. Res. Soc. Jpn.* 26-3 (2001) 1049.
- [15] C. Zener; *Phys. Rev.* 82 (1951) 403.
- [16] P. W. Anderson, H. Hasegawa; *Phys. Rev.* 100 (1995) 675.
- [17] P. -G. de Gennes; *Phys. Rev.* 118 (1960) 141.
- [18] M. Paraskevopoulos, F. Mayr, J. Hemberger, A. Loidl, R. Heichele, D. Maurer, V. Muller, A. A. Mukhin, A. M. Balbashov; *J. Phys.; Condens. Matter* 12 (2000) 3993.
- [19] G. P. Luo, Y. S. Wang, S. Y. Chen, A. K. Heilman, C. L. Chen, C. W. Chu, Y. Liou, N. B. Ming; *Appl. Phys. Lett.* 76-14 (2000) 1908.
- [20] R. Mallik, E. V. Sampathkumaran, P. L. Paulose; *Appl. Phys. Lett.* 71-16 (1997) 2385.
- [21] M. Uehara, S. Mori, C. H. Chen, S. -W. Cheong; *Nature* 399 (1999) 560.

(Received October 13, 2003; Accepted July 1, 2004)